

Discovery of SN 2009nz Associated with GRB 091127

B. E. Cobb¹, J. S. Bloom¹, D. A. Perley¹, A. N. Morgan¹, S. B. Cenko¹, and A. V. Filippenko¹

bcobb@astro.berkeley.edu

ABSTRACT

We report SMARTS, Gemini and *Swift*-UVOT observations of the optical transient (OT) associated with gamma-ray burst (GRB) 091127, at redshift 0.49, taken between 0.9 hr and 102 days following the *Swift* trigger. In our early-time observations, the OT fades in a manner consistent with previously observed GRB afterglows. However, after 9 days post-burst, the OT is observed to brighten for a period of ~ 2 weeks, after which the source resumes fading. A comparison of this late-time “bump” to SN 1998bw (the broad-lined Type Ic supernova associated with GRB 980425), and several other GRB supernovae (SNe), indicates that the most straightforward explanation is that GRB 091127 was accompanied by a contemporaneous SN (SN 2009nz) that peaked at a magnitude of $M_V = -19.0 \pm 0.2$. SN 2009nz is globally similar to other GRB supernovae, but evolves slightly faster than SN 1998bw and reaches a slightly dimmer peak magnitude. We also analyze the early-time UV-optical-IR spectral energy distribution of the afterglow of GRB 091127 and find that there is little to no reddening in the host galaxy along the line-of-sight to this burst.

Subject headings: gamma-ray burst: individual (GRB 091127) — supernovae: individual (SN 2009nz)

1. Introduction

The list of gamma-ray bursts (GRBs) that are associated with supernovae (SNe) has grown in the last decade (e.g., GRB 030329/SN 2003dh — Hjorth et al. 2003, Stanek et al. 2003, Bloom et al. 2004; GRB 031203/SN 2003lw — Cobb et al. 2004, Gal-Yam et al. 2004, Malesani et al. 2004, Thomsen et al. 2004; GRB 060218/SN 2006aj — Campana et al. 2006, Ferrero et al. 2006, Mirabal et al. 2006, Cobb et al. 2006a, and references therein; GRB

¹Department of Astronomy, University of California, Berkeley, CA 94720-3411

050525a — Della Valle et al. 2006a; see also Woosley & Bloom 2006), indicating that at least some (perhaps most) long-duration GRBs result from the core collapse of massive stars. However, as evidenced by the failure to detect SNe associated with two nearby long-duration GRBs (GRB 060505 at redshift $z = 0.0889$ and GRB 060614 at $z = 0.125$: Cobb et al. 2006b, Della Valle et al. 2006b, Fynbo et al. 2006, Gal-Yam et al. 2006, Xu et al. 2009), we do not yet have a complete understanding of the progenitors of long-duration GRBs and the apparent origin of the diversity of their associated SN properties. Long-duration GRB 091127 ($T_{90} = 7.1$ s, Troja et al. 2009), presented us with a new opportunity to investigate the GRB-SN connection.

GRB 091127 triggered the *Swift* Burst Alert Telescope (Gehrels et al. 2004) on 2009 Nov. 27 at 23:25:45 (UT dates are used throughout this paper; Troja et al. 2009). The prompt emission had a power-law index of 2.05 ± 0.07 (-0.4 to 7.5 s post-burst) and a fluence of $9.0 \pm 0.3 \times 10^{-6}$ erg cm^{-2} (15-150 keV) (Stamatikos et al. 2009). The *Swift* X-ray Telescope observed the X-ray afterglow with a photon spectral index of $1.98_{-0.14}^{+0.15}$ and absorption column of $9.8_{-3.1}^{+3.3} \times 10^{20}$ cm^{-2} (Evans et al. 2009).

Swift could not immediately slew to the burst due to Earth-limb constraints, but an optical transient (OT) was quickly identified using the robotic 2-m Liverpool Telescope (Smith et al. 2009). *Swift* Ultraviolet and Optical Telescope (UVOT, Roming et al. 2005) observations, beginning ~ 50 min post-burst, confirmed the existence of this OT at $\text{RA}_{\text{J2000}} = 02^{\text{h}}26^{\text{m}}19.89^{\text{s}}$, $\text{Dec}_{\text{J2000}} = -18^{\circ}57'08''.5$ (Immler et al. 2009).

Gemini-North Multi-Object Spectrograph (GMOS, Hook et al. 2004) and Very Large Telescope X-shooter spectra of the OT revealed emission features from the underlying host galaxy of the GRB at $z = 0.49$ (Cucchiara et al. 2009; Thoene et al. 2009). Because of this relatively low redshift, GRB 091127 was an excellent candidate for follow-up observations in search of a GRB-related SN.

In this *Letter*, we present optical data that show a late-time rebrightening in the OT of GRB 091127. We interpret this extra component of light as being due to a SN (SN 2009nz, Cobb et al. 2010) associated with GRB 091127. The observations, data reduction, and photometry are reported in §2. In §3, we consider each component of light associated with the OT and note the absence of reddening in the burst’s host galaxy. We conclude in §4 with a comparison of past GRB-SNe. Throughout this paper, we assume the standard cosmological model with $\Omega_{\Lambda} = 0.73$, $\Omega_m = 0.27$, and a Hubble constant of $71 \text{ km s}^{-1} \text{ Mpc}^{-1}$.

2. Observations, Data Reduction and Photometry

2.1. SMARTS Optical/IR Observations

We began observing the field of GRB 091127 on 2009 Nov. 28 at 01:15, ~ 1.8 hr post-burst (Troja et al. 2009), using ANDICAM (A Novel Dual Imaging CAMera) mounted on the Small and Moderate Aperture Research Telescope System (SMARTS)¹ 1.3-m telescope at Cerro Tololo Inter-American Observatory.² Initial SMARTS observations were obtained in short exposures over ANDICAM’s full wavelength range (*BVRIJHK*); as the OT faded, longer observations were obtained with fewer filters. A thorough analysis of the afterglow of GRB 091127, including the full-color SMARTS dataset, is available in Troja et al. (2010, in prep.). Over 11 epochs between 1.8 hr and 24 days post-burst, dithered images were obtained and then reduced and combined using standard IRAF³ tasks (see Table 1, Fig. 1).

The brightness of the OT of GRB 091127 was measured using seeing-matched aperture photometry relative to a set of on-chip, nonvariable sources. Relative magnitudes were converted to apparent magnitudes by comparison, on a photometric night, with Rubin 149 Landolt standard stars (Landolt 1992). In addition to the relative measurement error, there is a systematic error of 0.05 mag associated with the uncertainties in this photometric calibration. All photometry in this paper is corrected for a Galactic reddening of $E_{B-V} = 0.038$ mag (Schlegel et al. 1998).

2.2. Gemini Optical Observations

We obtained images of GRB 091127 using GMOS on the 8-m Gemini-South telescope. Five epochs of GMOS *i'*-band imaging were obtained between 9 and 102 days post-burst (see Table 1). Each set of Gemini images consisted of dithered exposures reduced and combined using the standard `gemini.gmos` IRAF package.

Seeing-matched, relative aperture photometry was performed on the OT of GRB 091127. The relative to apparent magnitude transformation utilized two stars common to both the SMARTS and Gemini images. The *i'*-band apparent magnitudes of the stars were determined

¹<http://www.astro.yale.edu/smarts>.

²<http://www.astronomy.ohio-state.edu/ANDICAM>.

³IRAF is distributed by National Optical Astronomy Observatory, which is operated by the Association for Research in Astronomy, Inc., under cooperative agreement with the NSF.

with the SDSS transformation equations of Jordi et al. (2006)⁴, utilizing the stars’ I - and R -band SMARTS magnitudes. These Gemini i' -band magnitudes were then transformed back into the I -band to match the SMARTS photometric system. While these transformations may introduce some systematic error into the Gemini photometry, they do not affect the relative magnitudes. The match between SMARTS and Gemini values measured at similar epochs suggests that no significant error has been introduced.

ISIS (Alard 2000) kernel-convolved image subtraction was carried out on the Gemini images (Fig. 2). The image obtained 102 days post-burst was used as the subtraction reference frame. Residual light is evident in each subtracted frame, indicating that the OT was dimmest in the final image. This is expected, of course, if the earlier images contain afterglow light. However, both the image subtraction and the photometry indicate that the transient *brightens* by 0.06 ± 0.02 mag between 9 and 18 days post-burst. As described in §3, we interpret this brightening to indicate the presence of an underlying GRB-SN.

2.3. UVOT Observations

UVOT observations of GRB 091127 began on 2009 Nov. 28 at 00:19:29, 53.65 min after the trigger, and the afterglow was detected in all utilized filters. Count rates were measured using 5" apertures on data taken with the U , $UVW1$, and $UVM2$ filters, and were calibrated using the UVOT Photometric System described by (Poole et al. 2008, see Table 1).

3. Data Analysis

The OT of GRB 091127 consists of three distinct sources of light. The first source is the steady contribution from the underlying host galaxy, which dominates at late times ($t_{\text{obs}} \gtrsim 50$ days). The second source, most important at early times ($t_{\text{obs}} \lesssim 6$ days), is the decaying optical afterglow (OAG) of the GRB. The third source is the rising and then decaying light from the putative SN associated with GRB 091127, SN 2009nz, which begins to contribute significantly to the system several days post-burst. Below, we consider each of these contributions in turn.

⁴<http://www.sdss.org/dr7/algorithms/sdssUBVRITransform.html#Jordi2006>.

3.1. Host Galaxy

We assume that in the final Gemini image (~ 102 days post-burst), all transient sources associated with GRB 091127 no longer contribute significantly to the observed optical flux. Therefore, we take the magnitude at that epoch ($I = 22.54 \pm 0.05$ mag) to be the brightness of the host. If a small contribution of extra light from the OAG or SN is still present in our images at this epoch, then we may have overestimated the brightness of the host; thus, we will have oversubtracted the host contribution and slightly underestimated the peak brightness of the GRB-SN associated with GRB 091127. We estimate that the systematic uncertainty in the SN peak brightness introduced by host-galaxy subtraction is < 0.1 mag.

3.1.1. GRB Position

The host galaxy of GRB 091127 exhibits a nonstellar radial profile (full width at half-maximum intensity $\sim 1''.0$ when the seeing was $0''.7$), with a slight elongation from northwest to southeast. The centroid of the OT is offset from the host-galaxy center by $0''.09 \pm 0''.01$ west and $0''.26 \pm 0''.01$ south. The position of the GRB is, therefore, inconsistent with the center of the galaxy. At the distance of the host ($z = 0.49$), $1''$ is 6.02 kpc in projection. Thus, the GRB occurred $\gtrsim 1.66 \pm 0.06$ kpc from the host center, which is a typical offset for a long-duration GRB (Bloom et al. 2002a; Fruchter et al. 2006).

3.1.2. Host-Galaxy Reddening

SMARTS observations were obtained with a cadence designed to ensure that the final combined frames in each filter are referenced to the same mid-exposure time. The *BVRIJHK* images obtained during the first SMARTS epoch have a common mid-exposure time of 2.2 hr post-burst. The OAG was brightest during this epoch, so we use these data to build the spectral energy distribution (SED) of the afterglow in order to evaluate whether there is significant extinction along the line-of-sight through the GRB host galaxy.

To help constrain the host reddening, we extend the SED blueward of the SMARTS *B*-band filter using *Swift*-UVOT ultraviolet observations. The UVOT light curve was best sampled in the *U* filter, and a power-law fit to the data yield a decay slope of $\alpha = 0.55 \pm 0.05$ (for $f_\nu \propto t^{-\alpha}$, where f_ν is the transient’s flux density and t is the time since the burst trigger), consistent with the decay rates inferred from SMARTS (Cobb 2009) and SkyNet/PROMPT (Haislip et al. 2009) observations at similar times. Assuming this decay rate, UVOT magnitudes were extrapolated to the common time of 2.2 hr post-burst ($U =$

16.45 ± 0.10 mag, $UVW1 = 16.22 \pm 0.10$ mag, $UVM2 = 16.08 \pm 0.10$ mag) in order to match the SMARTS epoch.

Figure 3 shows the SMARTS/UVOT SED of the OAG of GRB 091127. After correction for Galactic extinction, the observed UV-optical-IR SED was fit assuming an intrinsic power law affected by an extinction screen at the host redshift of 0.49. We examined several models, including Milky Way-like extinction, SMC-like extinction, and LMC-like extinction using the parameterization of Fitzpatrick (1999). The data were also fit to an unextinguished power law. Fits with a small amount of host-galaxy extinction were statistically acceptable, as was the fit to the unextinguished case. Given that the addition of host-galaxy extinction does not significantly improve the model fit, we suggest there is little to no significant extinction along the line-of-sight to GRB 091127. The 3σ upper limit on host-galaxy extinction is $A_V < 0.5$ mag. If a small amount of extinction is present in the host galaxy, we will slightly underestimate the peak brightness of the SN associated with GRB 091127.

3.2. Optical Afterglow

The decay of the OAG of GRB 091127 is modeled by a broken power law. During the first three epochs, the power-law decay index calculated from the SMARTS *I*-band observations is $\alpha = 0.54 \pm 0.02$. At ~ 0.3 days post-burst, the power law steepens to $\alpha = 1.29 \pm 0.03$. This decay index is similar to that reported in other optical filters (Haislip et al. 2009). Observations taken up to 6 days post-burst are dominated by the OAG. The transient’s behavior in later epochs, however, deviates significantly from this power-law decay.

This late-time deviation may, in part, be due to light from the underlying host galaxy, so we subtract the host-galaxy contribution (see Table 1). At early times, this subtraction has very little effect on the brightness of the transient, but it does slightly steepen the later-time decay rate of the afterglow to $\alpha = 1.52 \pm 0.03$. Despite this subtraction, the transient still does not behave as expected for a very late-time OAG. Instead of following a power-law decay, the transient *brightens*.

It is not uncommon for an afterglow to brighten, though this usually occurs during its early-time evolution during or immediately after the prompt phase of the GRB (Oates et al. 2009; Kann et al. 2007). Optical flaring is also relatively common and is generally attributed to refreshed shocks or reverse shocks (e.g., Greiner et al. 2009). The OAG of GRB 091127 shows no indications of significant brightening or flaring at early times (Haislip et al. 2009). The X-ray afterglow of GRB 091127 also shows no flaring activity at early times and does not deviate from a simple power-law decay when the OT brightens. The brightening occurs

several weeks post-burst and, therefore, cannot be easily attributed to GRB central-engine activity. When a late-time rebrightening with a similar timescale to that of GRB 091127 has been observed following a GRB (see Woosley & Bloom 2006 and references therein), the light curve “bump” has been attributed to a SN that occurred concurrently with the GRB.

3.3. SN 2009nz Associated with GRB 091127

To examine the late-time brightening component of GRB 091127, both the host galaxy and OAG contributions are subtracted (see Table 1, Fig. 1, *inset*). To account for possible errors, a range of subtractions was implemented assuming every possible permutation of a $\pm 3\sigma$ error on the host brightness and the afterglow model. This 3σ confidence region is shown as the gray area in the inset of Figure 1 and likely overestimates the actual errors on the SN associated with GRB 091127. Variations in the assumed host-galaxy magnitude most strongly affect the brightness of the late-time observations, while changes in the fit to the afterglow alter the earlier-time observations.

Regardless of the exact values assumed for the host galaxy and OAG subtraction, the classic rise and then decay of a SN is clear. The observed peak magnitude of SN 2009nz is $I = 22.3 \pm 0.2$ mag, which occurs at 22 ± 3 days post-burst. At the burst’s redshift of 0.49, this is equivalent to an absolute peak magnitude of $M_V = -19.0 \pm 0.2$ occurring at a rest-frame time of 15 ± 2 days post-burst. For these calculations, we have assumed that the K-correction of this GRB-SN is similar to that of the prototypical GRB-SN, SN 1998bw, and employ a time-dependent, generalized K-correction (Kim et al. 1996) that utilizes the spectra of SN 1998bw from Patat et al. (2001) and the photometry of Galama et al. (1998).

The observed I -band light curve of SN 1998bw at $z = 0.49$ is shown as a curve in the inset of Figure 1. The SN associated with GRB 091127 evolves faster than SN 1998bw, and reaches a slightly dimmer peak magnitude. This peak magnitude could be brighter if the SN has been reddened by its host galaxy; the 3σ upper limit on reddening is $A_V < 0.5$ mag and, therefore, extinction is unlikely to alter the peak magnitude by more than a few tenths of a magnitude.

Given the resemblance between SN 1998bw and the extra component of late-time light in GRB 091127, alternatives to the SN explanation for the source of this light are difficult to support. While it was initially speculated that some late-time GRB optical afterglow rebrightenings might be attributed to “dust echos” (e.g., Waxman & Draine 2000), later analysis concluded that these models could not fit the data and SNe were much more natural explanations (Reichart 2001). Furthermore, similar late-time “bumps” in the OAG light curves

of other GRBs (e.g., GRB 021211, Della Valle et al. 2003; GRB 050525a, Della Valle et al. 2006a) have been shown spectroscopically to be GRB-SNe. Hence, we consider our observations to be an extremely strong photometric case for a SN associated with GRB 091127.

4. GRB-SNe Comparison

We compare the absolute V -band light curve of SN 2009nz with other GRB-SNe whose SN light curves can be separated from their OAGs (SN 1998bw/GRB 980425, SN 2003dh/GRB 030329, SN 2003lw/GRB 031203, and SN 2006aj/GRB 060218; see Fig. 4). The GRB-SNe are globally very similar in terms of rise times and peak magnitudes. The GRB-SNe cluster fairly tightly in peak brightness, though SN 2003lw appears to be somewhat brighter than the others. The exact peak magnitude of SN 2003lw, however, depends on a large and uncertain amount of Galactic and host-galaxy extinction (e.g., Malesani et al. 2004). Depending on the reddening values assumed, SN 2003lw may be up to 0.5 mag dimmer than shown in Figure 4, thus making its peak brightness more in line with the other GRB-SNe. The light curve of SN 2003dh is also subject to some uncertainty because of the difficulty of separating the SN component of GRB 030329 from its very bright OAG (Deng et al. 2005).

A significant variation among the GRB-SNe is their rise times, with SN 2006aj peaking the fastest and SN 2003lw taking the longest time to peak. There appears to be a trend toward brighter GRB-SNe evolving more slowly than fainter GRB-SNe (Bloom et al. 2002b). For every 0.1 mag of dimming (brightening) compared to the peak brightness of SN 1998bw, the GRB-SNe evolve $6 \pm 2\%$ more quickly (slowly). This trend, however, has an unknown amount of associated error given the uncertainties associated with the light curves of SN 2003lw and SN 2003dh and the relative sparsity of V -band data points for SN 2003lw and, therefore, may not be significant (see Ferrero et al. 2006).

Considering the similarities in the light curves of SN 1998bw and SN 2009nz, it is likely that they ejected comparable amounts of ^{56}Ni ($0.5\text{--}0.7 M_{\odot}$, see Woosley & Bloom 2006 and references therein). The similarities between these two SNe are particularly interesting because of the large disparity between the gamma-ray energy associated with GRB 980425 and GRB 091127. GRB 980425 was a particularly subluminous GRB, with $E_{\text{iso}} \approx 10^{48}$ ergs, while GRB 091127 was a much more energetic burst with $E_{\text{iso}} \approx 10^{53}$ ergs (Stamatikos et al. 2009). Even if GRB 091127 was highly collimated, the gamma-ray energy output of GRB 091127 corrected for beaming is still at least a few orders of magnitude larger than that of GRB 980425. While there is evidence of a large population of local, low-energy, long-duration GRBs without significant OAGs that are associated with SN 1998bw-like SNe (see Cobb et al. 2006a), GRB 091127 with its large E_{iso} and bright OAG is not a member of

this class. Instead, GRB 091127 is much more similar to GRB 030329 (associated with SN 2003dh). The addition of another member to the class of GRB-SNe associated with “typical” energy, cosmological GRBs provides strong supporting evidence that many, if not most, long-duration GRBs are produced by the core collapse of massive stars.

We thank J. Espinoza, A. Miranda, and S. Tourtellotte for assistance with SMARTS observations (NOAO programs 2009B-0469/2010A-0113) and data reduction. B.E.C. acknowledges NSF Astronomy & Astrophysics Postdoctoral Fellowship AST-0802333. A.V.F. and S.B.C. acknowledge generous support from Gary & Cynthia Bengier, the Richard & Rhoda Goldman Fund, NASA/*Swift* grants NNX09AL08G/NNX10AI21G, and NSF AST-0908886. A.N.M. acknowledges support from an NSF Graduate Research Fellowship. The Gemini Observatory (data obtained under programs GS-2009B-Q-5/GS-2010A-Q-5) is operated by AURA under an agreement with the NSF on behalf of the Gemini partnership: the NSF (US), the Science and Technology Facilities Council (UK), the National Research Council (Canada), CONICYT (Chile), the Australian Research Council (Australia), Ministério da Ciência e Tecnologia (Brazil), and Ministerio de Ciencia, Tecnología e Innovación Productiva (Argentina). We acknowledge the use of public data from the *Swift* archive.

REFERENCES

- Alard, C. 2000, *A&AS*, 144, 363
- Bloom, J. S., Kulkarni, S. R., & Djorgovski, S. G. 2002, *AJ*, 123, 1111
- Bloom, J. S., et al. 2002, *ApJ*, 572, L45
- Bloom, J. S., van Dokkum, P. G., Bailyn, C. D., Buxton, M. M., Kulkarni, S. R., & Schmidt, B. P. 2004, *AJ*, 127, 252
- Campana, S., et al. 2006, *Nature*, 442, 1008
- Cobb, B. E., Bailyn, C. D., van Dokkum, P. G., Buxton, M. M., & Bloom, J. S. 2004, *ApJ*, 608, L93
- Cobb, B. E., Bailyn, C. D., van Dokkum, P. G., & Natarajan, P. 2006, *ApJ*, 645, L113
- Cobb, B. E., Bailyn, C. D., van Dokkum, P. G., & Natarajan, P. 2006, *ApJ*, 651, L85
- Cobb, B. E. 2009, GRB Coordinates Network, 10244

- Cobb, B. E., Bloom, J. S., Morgan, A. N., Cenko, S. B., Perley, D. A., 2010, Central Bureau Electronic Telegrams, 2288
- Cucchiara, A., Fox, D., Levan, A., Tanvir, N. 2009, GRB Coordinates Network, 10202
- Della Valle, M., et al. 2003, A&A, 406, L33
- Della Valle, M., et al. 2006, ApJ, 642, L103
- Della Valle, M., et al. 2006, Nature, 444, 1050
- Deng, J., Tominaga, N., Mazzali, P. A., Maeda, K., & Nomoto, K. 2005, ApJ, 624, 898
- Evans, P. A., et al. 2009, GRB Coordinates Network, 10201
- Ferrero, P., et al. 2006, A&A, 457, 857
- Fitzpatrick, E. L. 1999, PASP, 111, 63
- Fruchter, A. S., et al. 2006, Nature, 441, 463
- Fynbo, J. P. U., et al. 2006, Nature, 444, 1047
- Galama, T. J., et al. 1998, Nature, 395, 670
- Gal-Yam, A., et al. 2004, ApJ, 609, L59
- Gal-Yam, A., et al. 2006, Nature, 444, 1053
- Gehrels, N., et al. 2004, ApJ, 611, 1005
- Greiner, J., et al. 2009, ApJ, 693, 1912
- Haislip, J., et al. 2009, GRB Coordinates Network, 10219
- Hjorth, J., et al. 2003, Nature, 423, 847
- Hook, I. M., Jørgensen, I., Allington-Smith, J. R., Davies, R. L., Metcalfe, N., Murowinski, R. G., & Crampton, D. 2004, PASP, 116, 425
- Immler, S., et al. 2009, GRB Coordinates Network, 10193
- Jordi, K., Grebel, E. K., & Ammon, K. 2006, A&A, 460, 339
- Kann, D. A., et al. 2007, ApJ *submitted*, arXiv:0712.2186
- Kim, A., Goobar, A., & Perlmutter, S. 1996, PASP, 108, 190

- Landolt, A. U. 1992, *AJ*, 104, 340
- Malesani, D., et al. 2004, *ApJ*, 609, L5
- Mirabal, N., Halpern, J. P., An, D., Thorstensen, J. R., & Terndrup, D. M. 2006, *ApJ*, 643, L99
- Oates, S. R., et al. 2009, *MNRAS*, 395, 490
- Patat, F., et al. 2001, *ApJ*, 555, 900
- Poole, T. S., et al. 2008, *MNRAS*, 383, 627
- Reichart, D. E. 2001, *ApJ*, 554, 643
- Roming, P. W. A., et al. 2005, *Space Science Reviews*, 120, 95
- Schlegel, D. J., Finkbeiner, D. P., & Davis, M. 1998, *ApJ*, 500, 525
- Smith, R. J., et al. 2009, GRB Coordinates Network, 10192
- Stamatikos et al. 2009, GRB Coordinates Network, 10197
- Stanek, K. Z., et al. 2003, *ApJ*, 591, L17
- Thoene, C. C., et al. 2009, GRB Coordinates Network, 10233
- Thomsen, B., et al. 2004, *A&A*, 419, L21
- Troja, E., et al. 2009, GRB Coordinates Network, 10191
- Waxman, E., & Draine, B. T. 2000, *ApJ*, 537, 796
- Woosley, S. E., & Bloom, J. S. 2006, *ARA&A*, 44, 507
- Xu, D., et al. 2009, *ApJ*, 696, 971

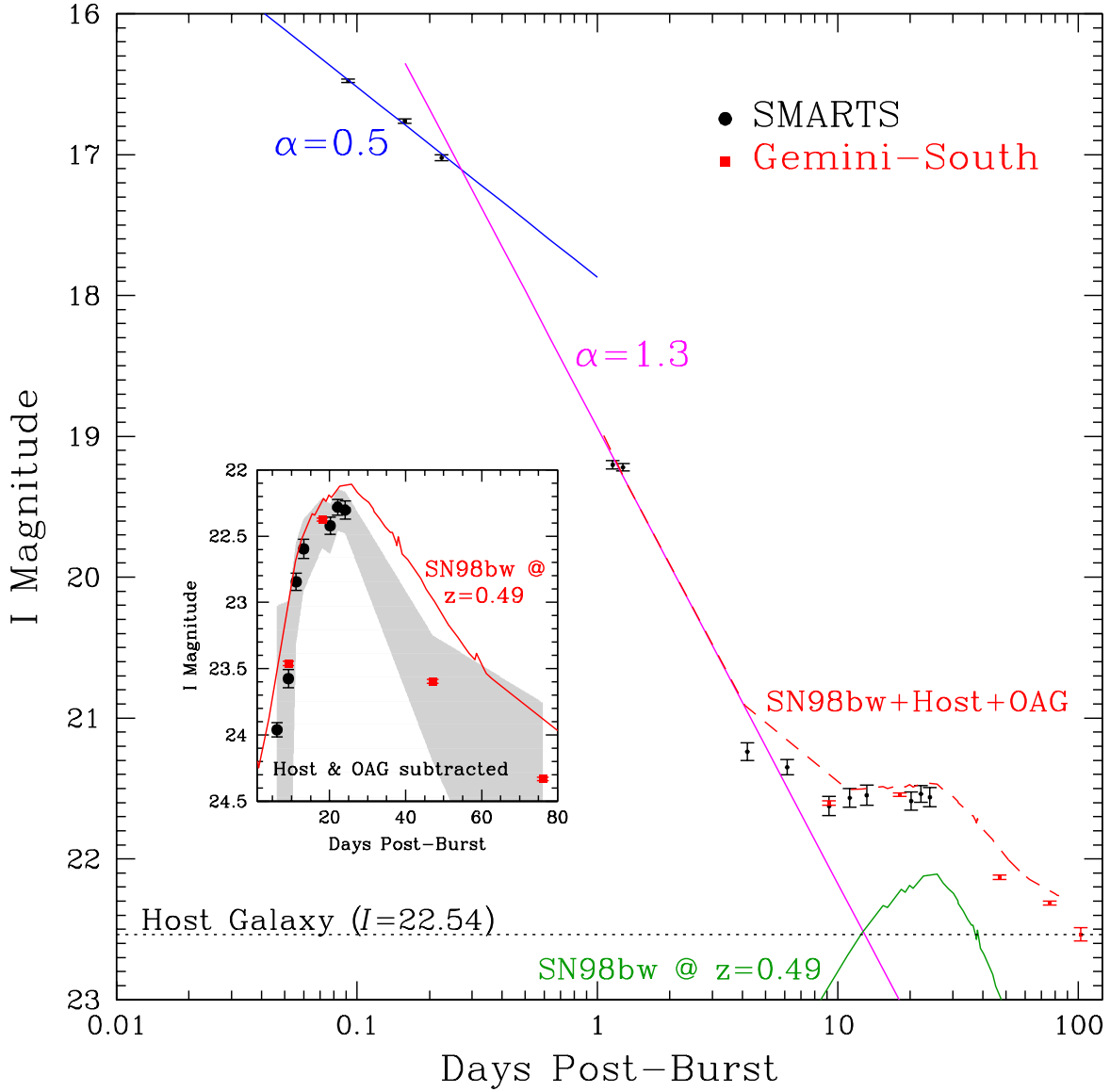


Fig. 1.— Observed I -band light curve of GRB 091127’s OT. The initial decay rate is $\alpha \approx 0.5$, which steepens to $\alpha \approx 1.3$ ($\alpha \approx 1.5$ after host-galaxy subtraction). The brightness of SN 1998bw at $z = 0.49$ is shown for comparison. Also shown is the light curve expected if a SN 1998bw-like SN had been associated with this burst’s host and OAG (SN98bw+Host+OAG) — this is brighter than the observed points, indicating that the GRB 091127 SN is slightly dimmer than SN 1998bw. *Inset:* An observer-frame comparison of SN 1998bw and the SN associated with GRB 091127. The points show the SMARTS/Gemini observations with both the host and the OAG contributions removed. The grey shaded region is the 3σ confidence region, allowing for possible errors in the magnitude of the host and the afterglow model. This SN evolves somewhat more quickly than SN 1998bw and peaks at a slightly dimmer magnitude.

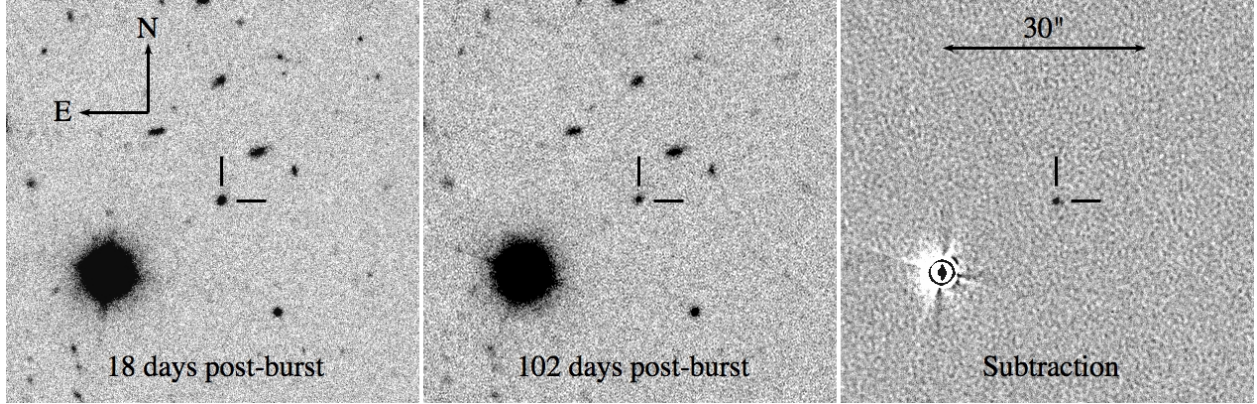


Fig. 2.— Gemini i' -band images of GRB 091127 taken at 18 days (*left*) and 102 days (*center*) post-burst. The position of the transient/host galaxy is indicated. The *right panel* shows the image subtraction of the two previous panels. Residual light is evident in the subtracted frame and is comprised of light from both the OAG and SN 2009nz.

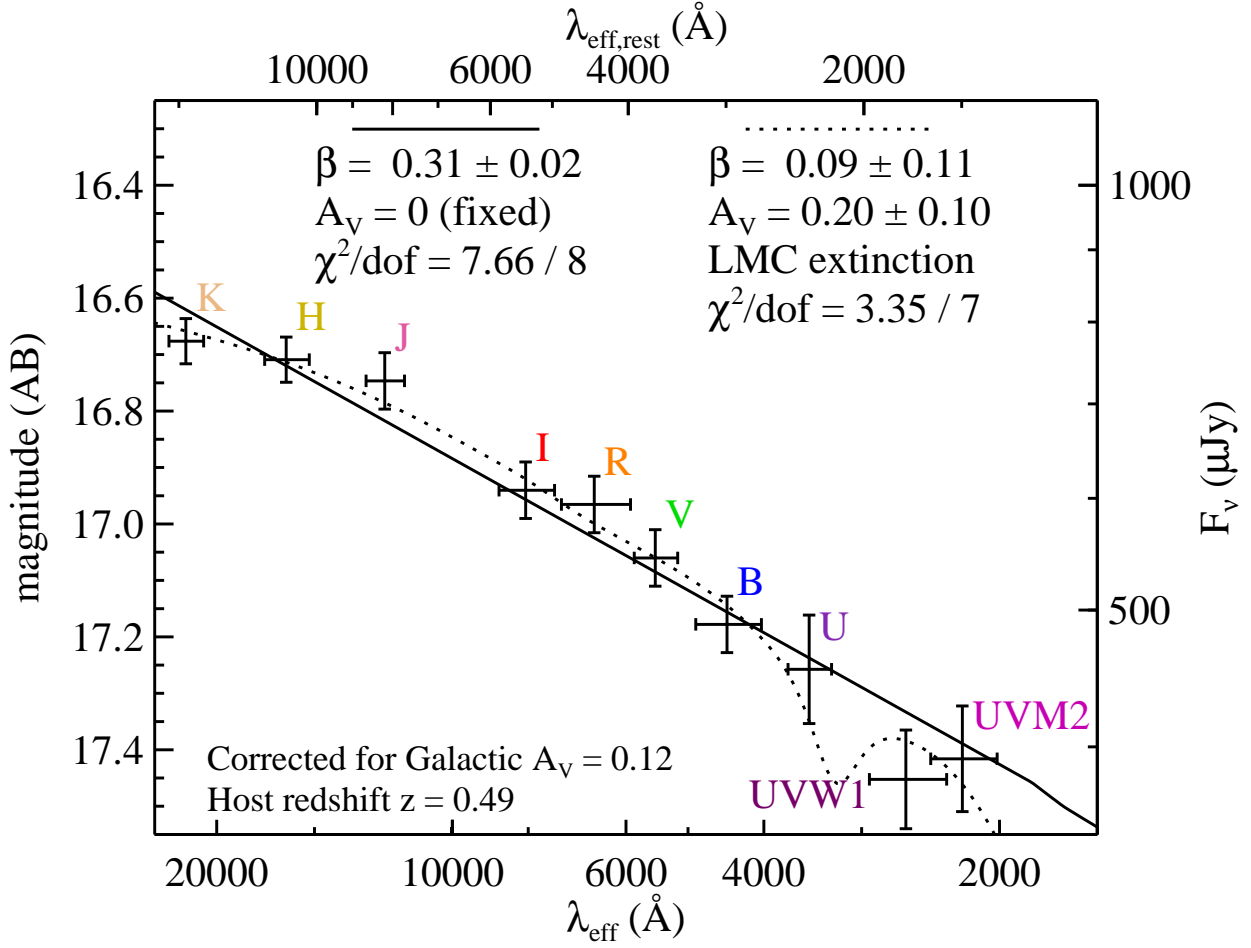


Fig. 3.— UV-optical-IR SED of the OAG of GRB 091127 at ~ 2.2 hr post-burst (corrected for Galactic extinction). The solid line shows a power-law fit assuming no host-galaxy extinction. The dotted line shows a fit using a model that includes a small amount of LMC-like extinction in the host. Both fits are statistically acceptable, indicating that there is little to no significant host-galaxy extinction along the line-of-sight to this GRB.

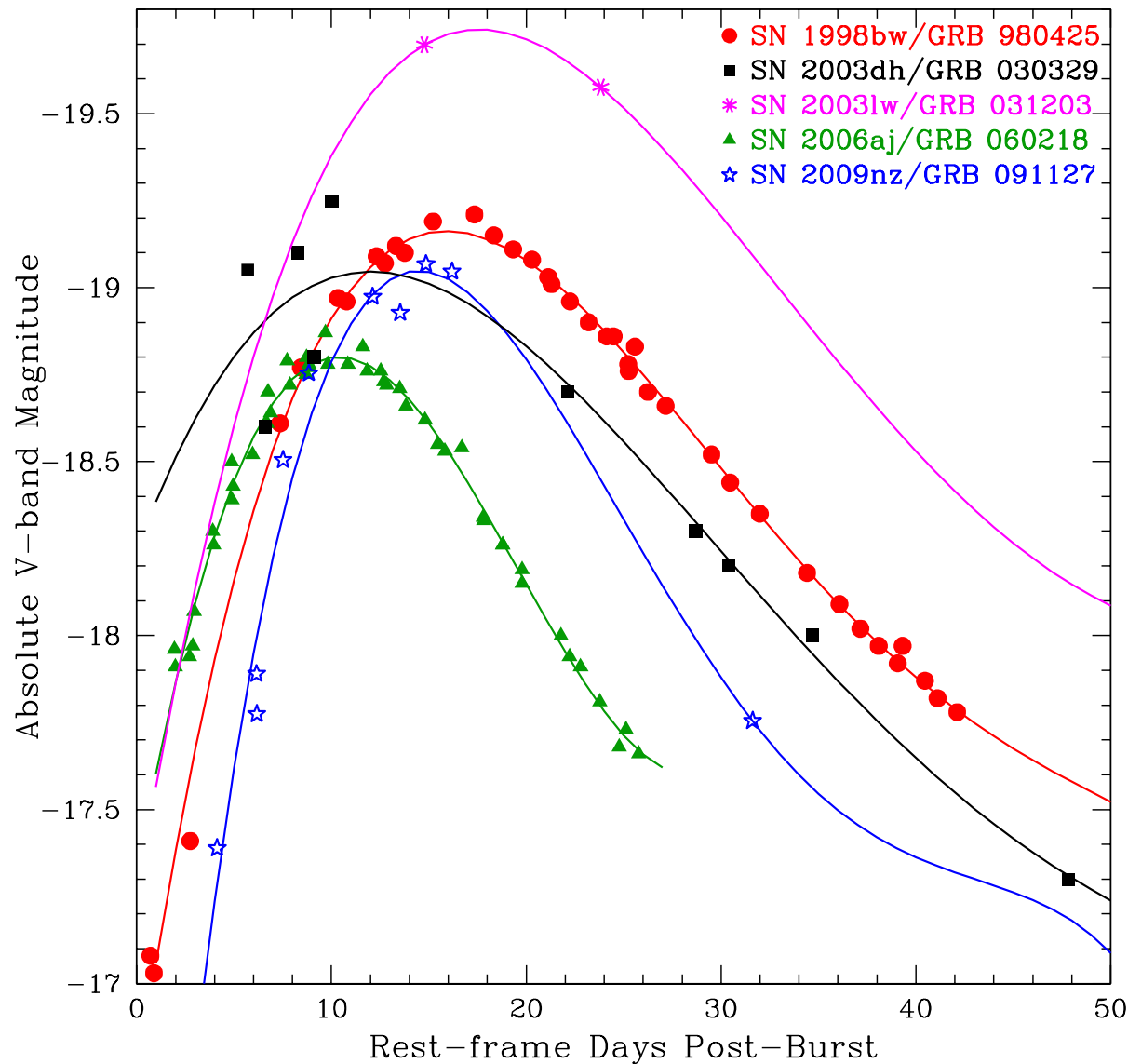


Fig. 4.— Comparison of GRB-SNe absolute V -band light curves, with data obtained from the following references: SN 1998bw, Galama et al. 1998; SN 2003dh, Deng et al. 2005; SN 2003lw, Malesani et al. 2004; SN 2006aj, Mirabal et al. 2006, and Ferrero et al. 2006. To guide the eye, the points have been fit with simple polynomial curves. GRB 031203 occurred behind a large and uncertain amount of Galactic and host-galaxy extinction and could, therefore, be as much as 0.5 mag dimmer.

Table 1. GRB 091127 Optical Transient Photometry

Observed Days ^a	Rest-Frame Days ^b	Magnitude ^c	Filter	Exp. Time (s)	Instrument	m_I OAG+SN ^d	m_I SN ^e	M_V SN ^f
0.04263	0.02861	15.64 ± 0.05	UVM2	196.6	<i>Swift</i> /UVOT
0.04410	0.02960	15.70 ± 0.07	UVW1	40.9	<i>Swift</i> /UVOT
0.06419	0.04308	16.01 ± 0.05	UVW1	115.2	<i>Swift</i> /UVOT
0.06713	0.04505	16.26 ± 0.13	U	10.6	<i>Swift</i> /UVOT
0.09183	0.06163	17.29 ± 0.01	B	180	SMARTS/ANDICAM
0.09183	0.06163	17.05 ± 0.01	V	120	SMARTS/ANDICAM
0.09183	0.06163	16.76 ± 0.01	R	180	SMARTS/ANDICAM
0.09183	0.06163	16.48 ± 0.01	I	180	SMARTS/ANDICAM	16.48
0.09183	0.06163	15.87 ± 0.03	J	180	SMARTS/ANDICAM
0.09183	0.06163	15.35 ± 0.03	H	120	SMARTS/ANDICAM
0.09183	0.06163	14.82 ± 0.03	K	180	SMARTS/ANDICAM
0.10804	0.07251	16.57 ± 0.02	U	542.9	<i>Swift</i> /UVOT
0.13365	0.08970	16.76 ± 0.11	U	25.4	<i>Swift</i> /UVOT
0.15803	0.10606	16.76 ± 0.02	I	180	SMARTS/ANDICAM	16.77
0.17632	0.11834	16.86 ± 0.02	U	819.6	<i>Swift</i> /UVOT
0.22483	0.15089	17.02 ± 0.02	I	180	SMARTS/ANDICAM	17.03
1.15758	0.77690	19.20 ± 0.03	I	1080	SMARTS/ANDICAM	19.25
1.27663	0.85680	19.22 ± 0.03	I	1080	SMARTS/ANDICAM	19.27
4.19824	2.81761	21.24 ± 0.06	I	2160	SMARTS/ANDICAM	21.63
6.15057	4.12790	21.35 ± 0.05	I	2160	SMARTS/ANDICAM	21.79	23.96	-17.39
9.17582	6.15827	21.60 ± 0.02	I	900	Gemini/GMOS	22.20	23.46	-17.89
9.18961	6.16752	21.63 ± 0.07	I	2160	SMARTS/ANDICAM	22.24	23.58	-17.78

Table 1—Continued

Observed Days ^a	Rest-Frame Days ^b	Magnitude ^c	Filter	Exp. Time (s)	Instrument	m_I OAG+SN ^d	m_I SN ^e	M_V SN ^f
11.19510	7.51349	21.57 ± 0.07	I	2160	SMARTS/ANDICAM	22.14	22.85	-18.51
13.16730	8.83711	21.55 ± 0.07	I	2160	SMARTS/ANDICAM	22.11	22.60	-18.75
18.05810	12.11950	21.55 ± 0.01	I	900	Gemini/GMOS	22.10	22.38	-18.97
20.16250	13.53190	21.59 ± 0.07	I	2160	SMARTS/ANDICAM	22.18	22.42	-18.93
22.13420	14.85520	21.54 ± 0.06	I	2160	SMARTS/ANDICAM	22.09	22.28	-19.07
24.12250	16.18960	21.56 ± 0.07	I	2160	SMARTS/ANDICAM	22.13	22.30	-19.05
47.10720	31.61560	22.13 ± 0.02	I	900	Gemini/GMOS	23.39	23.60	-17.76
76.11240	51.08210	22.31 ± 0.01	I	900	Gemini/GMOS	24.14	24.33	-17.02
102.03562	68.48030	22.54 ± 0.05	I	900	Gemini/GMOS

^aObserver frame days after burst trigger at 2009 Nov. 27, 23:25:45.

^bRest frame days after trigger; $t_{rest} = t_{obs}/(1+z)$.

^cVega magnitudes corrected for Galactic extinction ($E_{B-V} = 0.038$). In addition to the errors quoted, there is a systematic uncertainty of 0.05 mag in the SMARTS/Gemini photometric zero-point.

^dObserved I -band magnitude of the OT after subtraction of the host galaxy ($I_{host} = 22.54$ mag); it is a combination of the burst's OAG and SN.

^eObserved I -band magnitude of SN 2009nz. Both the host galaxy and the OAG have been subtracted from the raw observed magnitude of the OT. The brightness of the OAG is modeled by a fit 1–6 days post-burst (after

host subtraction), with OAG magnitude $=18.944 + 3.812 \times \log(t_{\text{obs}})$, where t_{obs} is days post-burst in the observer frame (column #1).

^fV-band absolute magnitude of SN 2009nz, assuming a distance modulus of 42.2 mag and a K-correction of -0.85 mag.